CHEMISTRY
A EUROPEAN JOURNAL

DOI: 10.1002/chem.200500605

Preparation, Characterization, and Application of Multistimuli-Responsive Microspheres with Fluorescence-Labeled Magnetic Cores and Thermoresponsive Shells

Yonghui Deng,[a] Changchun Wang,[a] Xizhong Shen,[b] Wuli Yang,[a] Lan Jin,[a] Hong Gao,[b] and Shoukuan Fu*[a]

Abstract: Novel functional microspheres with multistimuli-responsive properties have been prepared and characterized. The as-prepared microspheres respond to an external magnetic field, environmental temperature, and ultraviolet radiation. The in vitro drug-loading efficiency and drug-release behavior of these microspheres demonstrated that they could be used as drug carriers for drug controlled release. The results of in vivo distribution investigations of these microspheres showed that they exhibit a high magnetic-targeting effect, which holds promise for applications in various fields such as magnetic drug targeting and tissue labeling, among others.

Keywords: core–shell structures · drug carriers · fluorescence · magnetic properties · thermoresponsive

Introduction

Stimuli-responsive microspheres are microspheres that show an ability to change their physical-chemical properties and colloidal properties in response to environmental stimuli (change of temperature, pH, chemicals, light, electrical field, magnetic field, or mechanic stress, etc.). Such microspheres have been under intensive study in recent years as a result of their potential uses in biomedical and biotechnological fields such as controlled drug delivery,[1] biosensors,[2] chemical isolation,[3] cell-culture substrates,[4] enzyme immobilization,[5] bioelectrocatalysis,[6] and magnetically controlled electrochemical reactions.[7] A variety of stimuli-responsive microspheres have been reported, including pH-responsive,[8] thermoresponsive,[9] and magnetic microspheres,[10] among others; however, most of the reported stimuli-responsive microspheres only respond to one specific stimulus. For several of the potential applications of these microspheres, such as magnetically targeted drug delivery and magnetic isolation of chemicals, further functionalization of these magnetic microspheres is needed. When modified with a specific functional polymer, for example, a thermoresponsive polymer, these magnetic polymeric microspheres could be used to isolate chemicals more conveniently with the help of an external magnetic field, and by only changing the temperature of the sample solution. In addition, stimuli-responsive microspheres could be used in more extended domains if they are functionalized further.

Until now, to the best of our knowledge, only a little research has been directed towards the fabrication of microspheres that respond to more than one stimulus.[11] In this paper, based on our previous work,[12] to further endow stimuli-responsive microspheres with useful properties, we present the preparation of multistimuli-responsive microspheres that have a well-defined core–shell structure and multistimuli-responsive properties. For these microspheres, the core is made of FITC-labeled magnetic silica (FITC = fluorescein isothiocyanate) and the shell is made of cross-linked poly(*N*-isopropylacrylamide) (PNIPAM). FITC, a popular fluorescent probe, has been widely used in various fields such as cell labeling and DNA-sequence detection. PNIPAM is a well-known thermoresponsive polymer with a lower critical solution temperature (LCST) of 32 °C[9b] and has been extensively studied in many fields including drug delivery, purification of proteins, and gene expression. To further investigate the possible applications of the prepared multistimuli-responsive microspheres, we studied their drug-

[a] Y. Deng, Prof. C. Wang, Dr. W. Yang, L. Jin, Prof. S. Fu
Department of Macromolecular Science
Fudan University, Shanghai 200433 (China)
Fax: (+86) 21-6564-0293
E-mail: skfu@fudan.edu.cn

[b] Prof. X. Shen, Dr. H. Gao
Department of Gastroenterology, Zhongshan Hospital
Fudan University, Shanghai 200032 (China)

loading efficiency and in vitro drug-release behavior by using doxorubicin (DOX, a hydrophilic antitumor drug) as the model drug. In addition, by using these microspheres as tracers, we studied the magnetic-targeting effect of the microspheres by comparing the in vivo distribution of the microspheres in the presence and absence of an external magnetic field. The results suggest that such multistimuli-responsive microspheres, due to their photophysical and photochemical properties and sensitivity to both external magnetic field and environmental temperature, hold great potential for the design of controlled drug-delivery methods, in which microspheres loaded with a drug could be guided to the tissue of interest by using a magnetic field, followed by release of the drug by changing the local temperature. As a result of the enrichment of fluorescence molecules, these microspheres could serve as efficient tracers of drug carriers to study the magnetic-targeting effect of magnetic microspheres.

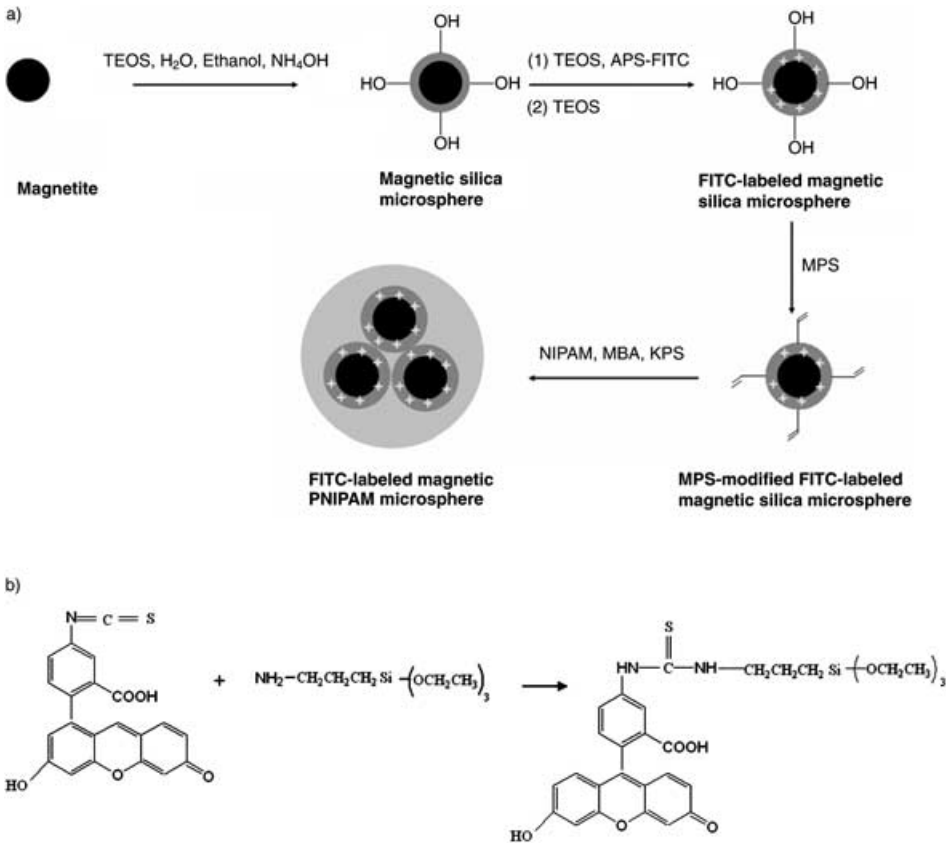

Figure 1. a) A schematic illustration for the preparation of a fluorescence-labeled magnetic thermoresponsive microsphere and b) the addition reaction between FITC and APS.

Results and Discussion

The concept of the proposed multistimuli-responsive microspheres and the fabrication procedure are schematically illustrated in Figure 1a. The first step in the procedure was to coat magnetite nanoparticles charged with citrate groups with a thin silica layer by using a modified Stöber method to give magnetic silica microspheres. Then, FITC molecules were incorporated into the silica layer of these microspheres by cohydrolysis of tetraethyl orthosilicate (TEOS) and APS–FITC compounds (APS = (3-aminopropyl)triethoxysilane) that had been synthesized beforehand by an addition reaction of APS and FITC (shown in Figure 1b). Subsequently, the resultant FITC-labeled magnetic silica microspheres were coated with another silica layer. In the next step, 3-(trimethoxysilyl)propyl methacrylate (MPS) was used to modify the surface of the FITC-labeled magnetic silica microspheres, which led to the formation of terminal C=C bonds on the surface of each microsphere core. Finally, in the presence of MPS-modified FITC-labeled magnetic silica microspheres, polymerization of *N*-isopropylacrylamide (NIPAM, the monomer) and *N*,*N*′-methylene bisacrylamide (MBA, the cross-linker) was initiated by using potassium persulfate (KPS) as an initiator. Uniform polymer shells were formed on the surface of the FITC-labeled magnetic silica microspheres, resulting in the formation of FITC-labeled magnetic PNIPAM microspheres.

Figure 2a shows the transmission electron microscopy (TEM) image of the magnetite particles used in the present study, showing that they are nanosized (ca. 15 nm) and well dispersed. The magnetite nanoparticles were synthesized by a chemical coprecipitation method of ferrous and ferric salts, followed by activation treatment with trisodium citrate. Figure 2b shows the TEM image of the magnetic silica microsphere nanoparticles, which clearly shows that the magnetite nanoparticles were fully coated by the silica. The TEM image shows that the size of the magnetic silica micro-

Abstract in Chinese:

摘要： 本文报道了一种同时具有磁响应性、热敏性的、发荧光的多重响应的新型功能微球。利用该微球作为药物载体的体外药物释放实验证明微球的药物释放具有温度可控性，另外，利用微球的磁性和荧光特性，发现微球在动物体内的磁靶向效果非常好，因此，该微球在药物控制释放、体内靶向性考察等领域具有广阔的应用前景。

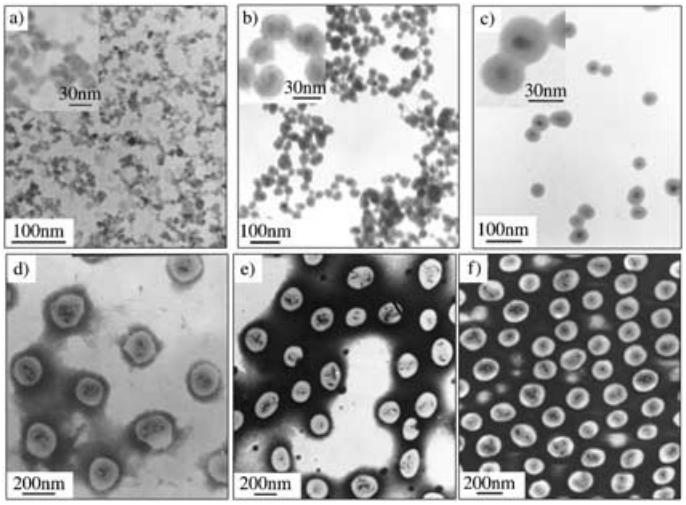

Figure 2. TEM image of a) colloidal magnetite nanoparticles, b) silica-coated magnetic nanoparticles, c) FITC-labeled magnetic silica microspheres, and FITC-labeled magnetic PNIPAM microspheres with a cross-linking density of d) 5%, e) 10%, and f) 15%.

spheres is about 30 nm. The silica coating on the magnetite particles not only protects the particles from dissolving in harsh application environments, but also provides a silica-like surface for further surface modification, such as that needed in the subsequent grafting or coating with a functional polymer. Magnetic microspheres labeled with fluorescence molecules could be used in many fields such as fluorescence magnetic markers in labeling and isolation of cells or biomacromolecules. To label the magnetic silica microspheres in this study, the FITC-APS compound was first synthesized in absolute ethanol by using an addition reaction involving the amino groups of APS and the isothiocyanate groups of FITC. The FITC molecules were then incorporated into the silica shells of magnetic silica microspheres by further cohydrolysis of TEOS and APS-FITC by means of a sol–gel approach. After incorporation of the FITC molecules into the silica layer of the microspheres, another addition of TEOS was required to form a new silica layer on these microspheres to avoid them aggregating as a result of the introduction of the FITC molecules. Xia's group successfully synthesized fluorescent iron oxide–silica nanoparticles with a method similar to that described here, by using surfactant-stabilized iron oxide nanoparticles as seeds.[13] Figure 1c shows the TEM image of FITC-labeled magnetic silica microspheres; this image suggests that core–shell microspheres (40–50 nm) with more regular morphology were prepared through a step-by-step coating procedure. It is worth noting that in this study, coating the magnetite nanoparticles was very necessary. As mentioned above, it provides magnetite nanoparticles with a silica-like surface which favors not only the introduction of FITC, but also the encapsulation of magnetite nanoparticles by polymers, as will be discussed below.

To further functionalize the FITC-labeled magnetic silica microspheres, various methods such as surface-initiation polymerization and precipitation polymerization can be used to coat their outer surfaces, resulting in a variety of functional polymeric shells. Before the coating procedure, modification of the silica layer surface is usually needed for the microspheres to be fully encapsulated by the polymers. In this study, MPS, a polymerizable silane coupling agent, was used to modify the surface of the FITC-labeled magnetic silica microspheres. By using the MPS-modified FITC-labeled magnetic microspheres as seeds, FITC-labeled magnetic PNIPAM microspheres were produced by precipitation polymerization of NIPAM and MBA. For comparison purposes, different weight ratios of MBA to NIPAM were used to prepare FITC-labeled magnetic PNIPAM microspheres with different cross-linking densities. Here, for convenience, the cross-linking density was defined as the weight percentage of cross-linker (MBA) to the monomer (NIPAM). Figure 2d,e,f are representative TEM images of FITC-labeled magnetic PNIPAM microspheres with different cross-linking densities, indicating that FITC-labeled core–shell magnetic silica microspheres were fully encapsulated by PNIPAM, and that FITC-labeled magnetic PNIPAM microspheres with an average diameter of about 200 nm were prepared. This TEM image shows that the cores of the resultant FITC-labeled magnetic PNIPAM microspheres contain several magnetic silica microspheres. This is probably due to the introduction of hydrophobic MPS on the magnetic silica microspheres, so these microspheres could not be fully dispersed in water, leading to their aggregated encapsulation by PNIPAM during the polymerization process. In addition, scanning electron microscopy (SEM) and atomic force microscopy (AFM) were used to determine the size and the morphology of the FITC-labeled magnetic PNIPAM microspheres. The SEM images in Figure 3a,b,c show that these microspheres have a narrow size distribution. Figure 3d is the AFM image of the prepared microspheres with a cross-

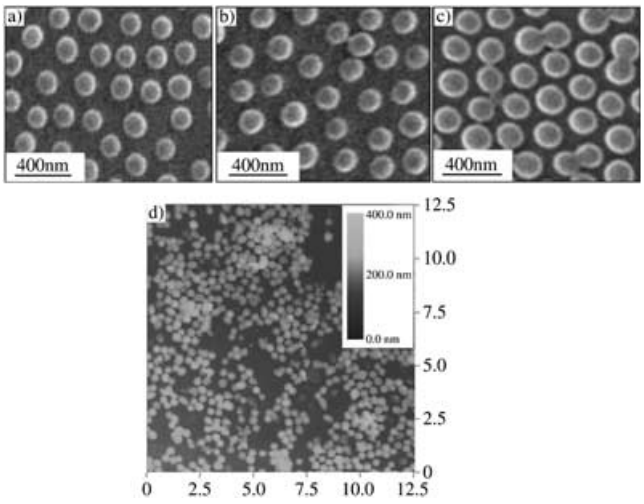

Figure 3. SEM image of FITC-labeled magnetic PNIPAM microspheres with a cross-linking density of a) 5%, b) 10%, and c) 15%, and d) AFM image (12.5×12.5 μm tapping mode) of FITC-labeled magnetic PNIPAM microspheres with a cross-linking density of 15%.

linking density of 15%, providing additional evidence that FITC-labeled magnetic PNIPAM microspheres with narrow size distribution were produced.

To investigate their thermoresponsive properties, dynamic light scattering (DLS) experiments were used to determine the temperature-induced dimensional change of FITC-labeled magnetic PNIPAM microspheres with different cross-linking densities (shown in Figure 4). According to the DLS results, all the synthesized microspheres exhibit a narrow

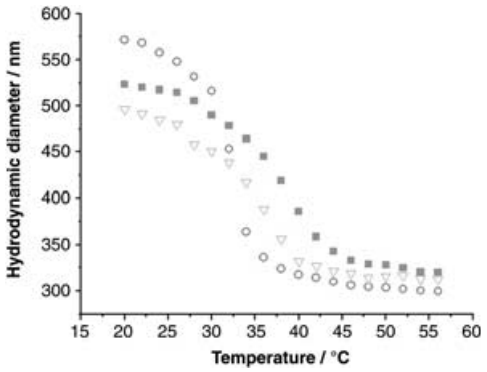

Figure 4. Temperature dependence of the hydrodynamic diameter of FITC-labeled magnetic PNIPAM microspheres with cross-linking density of 5% (○), 10% (■), and 15% (▽).

size distribution with a polydispersity index (PDI $= <\mu_2> / I^2$)[14] of less than 0.087, and as expected, they all exhibit thermoresponsive continuous volume phase-transition characteristics, except that microspheres with a lower cross-linking density (5%) display a sharper phase-transition curve than those with higher cross-linking densities (10% and 15%). It was also found that the LCST of FITC-labeled magnetic PNIPAM microspheres shifted from about 32 to 37°C when the cross-linking density increased from 5 to 15%. Such a shift was probably caused by the higher cross-linking density, which was also found by other authors studying cross-linked PNIPAM microspheres.[15] Furthermore, it was found that the dimensions of the microspheres decreased dramatically as the temperature increased. According to the DLS results, the swelling ratio (defined as $(D_{20°C}/D_{56°C})^3$, D = hydrodynamic diameter) of the microspheres decreased from 6.95 to 4.37 to 4.00 upon increasing the cross-linking density from 5 to 10 to 15%. As can be seen from the above discussion, the cross-linking density plays a critical role in the swelling and deswelling behavior of the microsphere, which is very important when considering applications in the fields of biology and medicine. Therefore, to prepare FITC-labeled magnetic PNIPAM microspheres with a certain LCST and swelling ratio, an appropriate amount of cross-linker (MBA) should be used.

To study the magnetic properties of the FITC-labeled magnetic PNIPAM microspheres, we recorded the hysteresis loop of the dried samples at room temperature. Figure 5 shows a characteristic magnetization curve of the sample, which indicates that FITC-labeled magnetic PNIPAM microspheres are superparamagnetic, that is, when the applied magnetic field is removed, the sample keeps no remanence. The superparamagnetism of the sample suggests that nanosized magnetite particles remain in the microspheres after being encapsulated by silica and PNIPAM. The superparamagnetism of magnetic microspheres is critical for their application in biomedical and bioengineering fields, as it prevents microspheres from aggregating and enables them to redisperse rapidly when the magnetic field is removed.[16] The inset in Figure 5 shows the separation and redispersion process of the microspheres in distilled water. In the absence of an external magnetic field, a dark yellow and homogeneous dispersion exists. When an external magnetic field was applied, magnetic PNIPAM microspheres were enriched and the dispersion became clear and transparent.

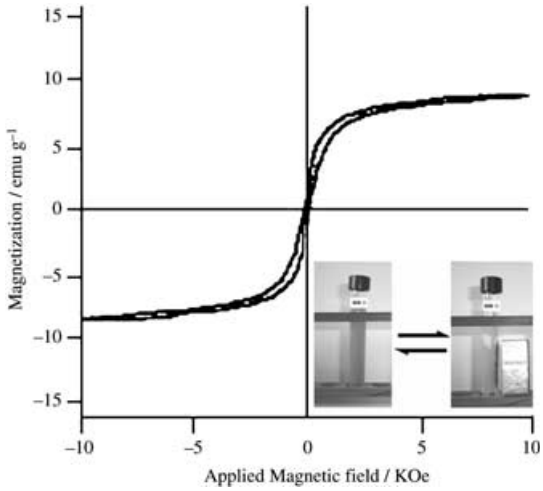

Figure 5. Magnetization curve of FITC-labeled magnetic PNIPAM microspheres with a cross-linking density of 15%. The inset shows the separation and redispersion process of the microspheres in distilled water in the absence (left) and presence (right) of an external magnetic field.

The incorporation of FITC molecules into the magnetic PNIPAM microspheres resulted in a value-added multistimuli-responsive microsphere which is of both fundamental and technological interest. When labeled with FITC, magnetic PNIPAM microspheres could be used as tracers for targeted drug controlled delivery under the guidance of a magnetic field. Because the PNIPAM shell of the microspheres showed a rapid swelling–deswelling transition with a simultaneous hydrophilic–hydrophobic transition, it would enhance the interaction between these microspheres and the tissue/organ of interest if the temperature was higher than the LCST of these microspheres. Figure 6 shows the fluorescence microscopy image of FITC-labeled magnetic PNIPAM microspheres. This figure shows that the luminescent intensity is high and the shining microspheres disperse very well. To further study the fluorescence property of the microspheres, the fluorescence emission spectra of FITC, FITC-labeled magnetic silica microspheres, and FITC-labeled magnetic PNIPAM microspheres with a cross-linking density of 15% were recorded (Figure 7). All samples were

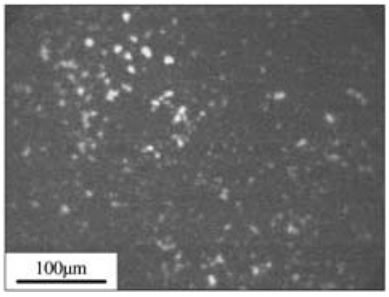

Figure 6. A fluorescence microscopy image of FITC-labeled magnetic PNIPAM microspheres with a cross-linking density of 15%.

measured using absolute ethanol as a dispersant. The fluorescence spectra showed that the emission maximum (λ_{max}) of both FITC-labeled magnetic silica microspheres and

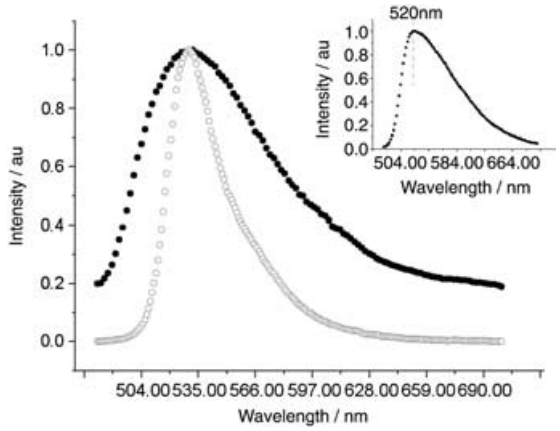

Figure 7. Normalized fluorescence emission spectra of FITC (■ shown in the inset, $[FITC] = 5.0 \times 10^{-6}$ mol L^{-1}), FITC-labeled magnetic silica microspheres (○, 2.0×10^{-3} g mL^{-1}), and FITC-labeled magnetic PNIAM microspheres (●, 15% cross-linking density, 5.0×10^{-3} g mL^{-1}). The samples were dispersed in absolute ethanol and exited at 470 nm.

FITC-labeled magnetic PNIPAM microspheres is about 530 nm, a redshift of 10 nm compared with that of free FITC (~520 nm). Red shifts were probably caused by the interactions between neighboring FITC molecules encapsulated by the silica matrix as a result of enrichment by magnetic silica microspheres, which was also reported by previous authors.[17] A quantitative calculation of the number of FITC molecules incorporated on each microsphere was difficult to obtain due to the fact that the silica-coated magnetite nanoparticles used for encapsulation of the FITC-APS compounds were not homogeneous in shape or size and the FITC-labeled magnetic silica microspheres were encapsulated in PNIPAM as aggregates of different sizes; however, the successful fabrication of FITC-labeled magnetic PNIPAM microspheres is clearly evident from both the fluorescence optical microscopy observation and fluorescence emission spectra of the samples.

As a consequence of the presence of the PNIPAM shell, the magnetic microspheres should swell and absorb DOX in aqueous solution, and by using a magnetic isolation process, the drug-loaded magnetic microspheres should be easily collected from the solution. In order to study the application possibilities, the prepared magnetic microspheres of 15% cross-linking density were used as matrices for loading and release of DOX. Drug loading was carried out by swelling a known weight of the dried microspheres in a solution of DOX in phosphate buffer (pH 7.4) at 27°C for 24 h. Figure 8a shows the resulting solution containing the micro-

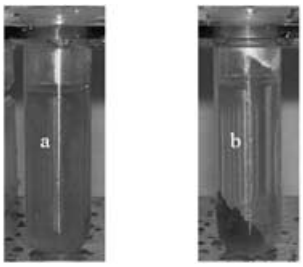

Figure 8. The suspension of FITC-labeled multiresponsive microspheres (15% cross-linking density) in phosphate buffer (pH 7.4) containing DOX a) before magnetic separation and b) after magnetic separation.

spheres (cross-linking density of 15%) and Figure 8b depicts the sample after separation with a magnetic field, which shows that DOX was enriched by the magnetic microspheres. The increase in the weight of the magnetic microspheres was taken as the amount of drug loaded, whereas no weight change was observed in phosphate buffer. Furthermore, for the confirmation of the percentage of drug loading in the microspheres, the amount of DOX left in the loading medium was determined by using a UV-visible spectrophotometer in accordance with Sampath and Robinson's method.[18] Table 1 summarizes the feeding ratios and drug-

Table 1. The feeding ratios and drug-loading efficiency (DLE) and drug-entrapment efficiency (DEE) of the magnetic microspheres studied.

$R_{DOX/microsphere}$[a]	DLE [%]	DEE [%]
0.5	18.5	45.4
1.0	23.4	30.4
2.0	25.8	17.3

[a] $R_{DOX/microsphere}$ represents the weight ratio of DOX to the magnetic microspheres (15% cross-linking density).

loading efficiency (DLE) of the magnetic microspheres. From the data in Table 1 it was found that an increase of $R_{DOX/microsphere}$ leads to a higher DLE, but it results in a decrease of drug-entrapment efficiency (DEE), that is, it lowers the utilization percentage of DOX. The enrichment of DOX in the magnetic microspheres was probably attributable to physical absorption.

For the drug-release studies, DOX-loaded (23.4%) magnetic microspheres were used to investigate their release be-

havior in water. Figure 9 depicts the cumulative percentage release of DOX from magnetic microspheres at different temperatures. Each point in the graph represents the mean value of the cumulative concentrate of released DOX, determined three times in the period when the temperature of the solution was kept constant. The drug-release profile can be divided into four zones, that is, 27–29 °C (A), 29–35 °C (B), 35–39 °C (C), and after 39 °C (D) (Figure 9). In zone A,

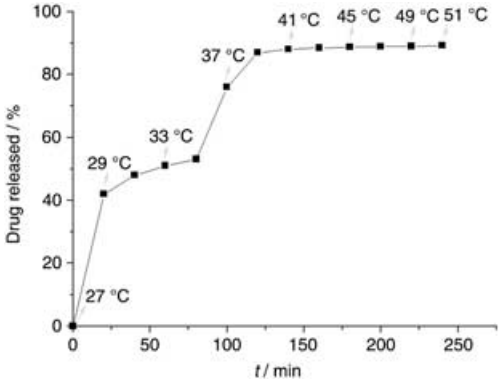

Figure 9. The DOX-release curve of DOX-loaded FITC-labeled multiresponsive microspheres (15% cross-linking density) in phosphate buffer (pH 7.4) at different temperatures.

a rapid release of the drug (ca. 41.7%) from the microspheres was observed. This is considered as a burst effect and is probably due to the desorption of DOX on the surface of the outer polymer shell, resulting from a large concentrate gradient between the aqueous solution and the interface of the drug-loaded microspheres. In zone B, with the increase of solution temperature, the polymer shell of the microspheres shrank gradually and, together with solubilized DOX, water in the polymer network was slowly expelled, leading to the drug-release percentage increasing gradually as the solution temperature was increased. Similarly, in zone C, the release percentage increases quickly upon increasing the temperature. It is worth noting that, as a result of rapid volume shrinkage of the microspheres around 37 °C, the total release percentage in zone C (ca. 34.0%) is larger than that of zone B (11.0%), and zone D shows only a little change in drug-release percentage (ca. 2.2%). As can be seen from Figure 7, the drug-release behavior of DOX-loaded magnetic microspheres shows a typical thermosensitive property on the whole.

By utilization of the fluorescent property and magnetic response of the FITC-labeled multiresponsive microspheres, the in vivo distribution analysis of these microspheres was conducted with a rabbit as the model animal. As shown in Figure 10 (left), when no external magnetic field was applied to the rabbit, fluorescence was observed under a fluorescence microscope in almost all visceral organ samples, such as the liver, spleen, lung, kidney, and heart, particularly in spleen and lung due to the presence of the reticuloendothelial system (RES). When an external magnetic field was applied at the position of the liver, fluorescence was observed

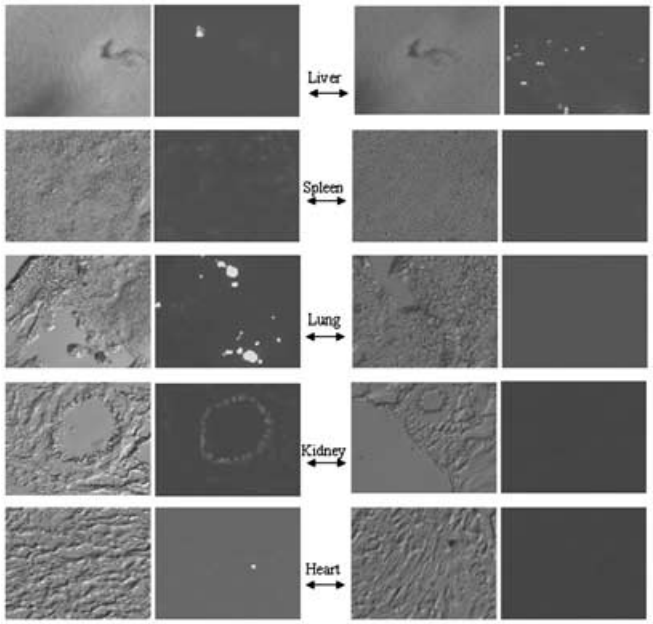

Figure 10. The fluorescence photographs of different tissue sections of test rabbit with no external magnetic field (left) and with an external magnetic field at the liver (right).

only in the liver and no fluorescent microspheres were found in the other visceral organs (see Figure 10 right). The results reveal that these microspheres could be used to study magnetic-targeting effects of magnetic microspheres conveniently.

Conclusion

In summary, we describe a simple and convenient method for the preparation of FITC-labeled magnetic PNIPAM microspheres which possess a well-defined core–shell structure and show multistimuli-responsive properties. The in vitro test results of DOX loading and release in the microspheres show that these microspheres hold great potential for controlled drug-release applications. The in vivo distribution analysis of the microspheres demonstrates that they could be conveniently used to study the magnetic-targeting effect of magnetic microspheres. The combined properties of such multistimuli-responsive microspheres make them promising for various applications, such as targeted drug delivery, separation of biomacromolecules, and cell and protein labeling.

Experimental Section

Preparation of colloidal magnetite nanoparticles: The colloidal magnetic nanoparticles were prepared by using the method already described,[19] based on the coprecipitation of $FeCl_2$ and $FeCl_3$ under a nitrogen atmosphere by adding a concentrated solution of sodium hydroxide (10 M) to the iron salts mixture (molar ratio $Fe^{2+}/Fe^{3+} = 1:2$). The prepared magnetic particles were dispersed in water, and the dispersion was adjusted to 4.0 wt% for further use.

Preparation and modification of FITC-labeled magnetic silica microspheres: The preparation and modification of the FITC-labeled magnetic silica microspheres were carried out at room temperature and involved three main steps. Firstly, an aqueous dispersion of magnetite nanoparticles (3.00 g, 4.0 wt%) charged with trisodium citrate was dispersed into a mixture of doubly distilled water (40 mL), ethanol (160 mL), and aqueous ammonia (5 mL, 30 wt%). Then, TEOS (0.5 mL) was added under continuous mechanical stirring, and the reaction was allowed to proceed for 12 h to produce the silica-coated magnetite nanoparticles. In the next step, FITC-labeled magnetic silica microspheres were produced by using the strategy developed by Van Blaaderen et al.[20] Briefly, APS (0.190 g) was added to a solution of FITC (0.037 g) in ethanol (10 mL). After stirring for 12 h, the resultant solution together with TEOS (0.5 mL) was added to the above-mentioned mixture containing the silica-coated magnetite nanoparticles, and the reaction was allowed to proceed for another 12 h. After this step, to promote the stability of the resultant FITC-labeled magnetic silica microspheres, an additional amount of TEOS (0.5 mL) was added to form another silica layer on the surface of the microspheres. Finally, to endow the surface of the FITC-labeled magnetic silica microspheres with reactive C=C bonds, MPS (4 mL) was added to the mixture and the reaction was allowed to proceed for 48 h. After surface-modification treatment, the MPS-modified FITC-labeled magnetic silica microspheres were collected by magnetic separation followed by washing several times with ethanol and then water. Then, doubly distilled water was added to achieve a dispersion of the obtained colloidal particles of 2.0 wt%.

Preparation of FITC-labeled magnetic PNIPAM microspheres: The resulting MPS-modified FITC-labeled magnetic silica microspheres dispersion was used for the precipitation polymerization of NIPAM and MBA by using KPS as the initiator. Under continuous mechanical stirring, the polymerization was carried out at 70°C for 4 h under a nitrogen atmosphere. A typical method for the preparation of FITC-labeled magnetic PNIPAM microspheres is as follows: an MPS-modified FITC-labeled magnetic silica microspheres dispersion (3.0 g, 2.0 wt%), NIPAM aqueous solution (2.00 g, 3.0 wt%), MBA aqueous solution (2.0 g, 0.3 wt%), KPS aqueous solution (1.0 g, 0.3 wt%), and doubly distilled water (40.0 g). The obtained FITC-labeled magnetic PNIPAM microspheres were washed with doubly distilled water repeatedly, and then enriched with the help of a magnet. All procedures associated with the preparation of FITC-labeled magnetic PNIPAM microspheres were performed in the dark to avoid bleaching.

Characterization: TEM images of magnetite nanoparticles, FITC-labeled magnetic silica microspheres, and FITC-labeled magnetic PNIPAM microspheres were obtained by using a Hitachi HU-11B transmission electron microscope. The samples of the FITC-labeled magnetic PNIPAM microspheres were stained by using phosphotungstic acid. AFM (Digital instruments Nanoscope III, USA) and SEM (Philips XL30) analyses were used to determine the size and the morphology of FITC-labeled magnetic silica microspheres and FITC-labeled magnetic PNIPAM microspheres. DLS analysis (Malvern 4700) was used to measure the hydrodynamic diameter of the FITC-labeled magnetic PNIPAM microspheres. A vibrating-sample magnetometer (VSM, EG&G Princeton Applied Research Vibrating Sample Magnetometer, Model 155, USA) was used at room temperature to characterize the magnetic properties of FITC-labeled magnetic PNIPAM microspheres. Fluorescence microscopy (Axiovert 200, Zeiss, Germany) was used to observe the images of FITC-labeled magnetic microspheres. Fluorescence emission spectra of the dilute samples in ethanol were recorded with a FLS920 model, Edinburgh Instruments.

Loading and release of DOX in FITC-labeled magnetic PNIPAM microspheres

Loading: Three different amounts of DOX powder (2.5, 5.0, and 10.0 mg) were dissolved in phosphate buffer (pH 7.4, 10 mL) to form aqueous DOX solutions (0.25, 0.50, and 1.00 mg mL^{-1}, respectively). Then, each solution was fully mixed with a suspension of microspheres (10 mL, 0.50 mg mL^{-1}, cross-linking density 15%) that had been prepared in advance. After incubation for 24 h at 27°C, the microspheres were collected by magnetic separation and were further dried under vacuum at 27°C, and the samples were denoted as samples A, B, and C, respectively.

Release: Typically, in a flask containing phosphate buffer (pH 7.4, 40 mL), sample B (0.50 mg) was dispersed at 27°C and a homogeneous suspension was obtained. Then, the suspension temperature was increased to 29°C at a rate of 1°C min^{-1}, and the temperature of the suspension was kept at 29°C for 20 min. 4.0 mL of the suspension was withdrawn from the flask and magnetically isolated, and the DOX concentrate in the supernatant was measured by using a UV/Vis spectrophotometer (Varian, Cary-100) at 482 nm. After the measurement, the withdrawn suspension was added back to the flask. The determination of DOX released in the suspension was repeated three times and a cumulative concentrate value of released DOX was obtained. Similarly, the mean cumulative concentrate values of released DOX at other temperatures were measured and the DOX-release curve of the drug-loaded magnetic microspheres was obtained.

Investigation of in vivo distribution of FITC-labeled magnetic PNIPAM microspheres: The FITC-labeled magnetic PNIPAM microspheres suspended in saline water (0.9 wt%) were introduced to the bodies of two white rabbits through a femoral artery injection according to a weight ratio of 10.00 mg microspheres per kg of body weight. For comparison, a button magnet (magnetic field strength of 1000 G) with a diameter of 1.5 cm and a thickness of 0.5 cm was posited at the liver of one of the test rabbits. After 2 h, the main visceral organs, including the liver, spleen, lung, kidney, and heart, were removed and sliced on a freezing microtome, and the slices of every visceral organ were observed under a fluorescence microscope to obtain the distribution of the microspheres.

Acknowledgements

The authors are grateful to the support of the National Science Foundation of China (NSFC, No. 20374012 and No. 50403011) and the Science and Technology Commission of Shanghai Municipality (STCSM, No. 03JC14012).

[1] a) P. K. Gupta, C. T. Hung, *Life Sci.* **1989**, *44*, 175; b) I. C. Kwon, Y. H. Bae, S. W. Kim, *Nature* **1991**, *354*, 291; c) H. Ichikawa, Y. Fukumori, *J. Controlled Release* **2000**, *63*, 107; d) N. Murthy, Y. X. Thng, S. Schuck, M. C. Xu, J. M. Frechet, *J. Am. Chem. Soc.* **2002**, *124*, 12398; e) H. Vihola, A. Laukkanen, J. Hirvonen, H. Tenhu, *Eur. J. Pharm. Sci.* **2002**, *16*, 69; f) A. Kikuchi, T. Okano, *Adv. Drug Delivery Rev.* **2002**, *54*, 53–77.

[2] a) Z. B. Hu, Y. Y. Chen, C. J. Wang, Y. D. Zheng, Y. Li, *Nature* **1998**, *393*, 149; b) H. van der Linden, S. Herber, W. Olthuis, *Sens. Mater.* **2002**, *14*, 129; c) Y. Weizmann, F. Patolsky, E. Katz, I. Willner, *J. Am. Chem. Soc.* **2003**, *125*, 3452; d) J. M. Perez, F. J. Simeone, Y. Saeki, L. Josephson, R. Weissleder, *J. Am. Chem. Soc.* **2003**, *125*, 10192; e) B. Panchapakesan, D. L. Devoe, M. R. Widmaier, *Nanotechnology* **2001**, *12*, 336.

[3] a) H. Kawaguchi, K. Fujimoto, *Bioseparation* **1998**, *7*, 253; b) A. Kondo, T. Kaneko, K. Higashitani, *Biotechnol. Bioeng.* **1994**, *44*, 1.

[4] a) O. H. Kwon, A. Kikuchi, M. Yamato, Y. Sakurai, T. J. Okano, *J. Biomed. Mater. Res.* **2000**, *50*, 82; b) L. K. Ista, V. H. Perez-Luna, G. P. Leopez, *Appl. Environ. Microbiol.* **1999**, *65*, 1603.

[5] A. Guiseppi-Elie, N. F. Sheppar, S. Brahim, D. Narinesigh, *Biotechnol. Bioeng.* **2001**, *75*, 475.

[6] a) E. Katz, I. Willner, *J. Am. Chem. Soc.* **2002**, *124*, 10290; b) D. E. Bergbreiter, B. L. Case, Y. S. Liu, J. W. Caraway, *Macromolecules* **1998**, *31*, 6053.

[7] E. Katz, R. Baron, I. Willner, *J. Am. Chem. Soc.* **2005**, *127*, 4060.

[8] a) M. Sauer, D. Streich, W. Meier, *Adv. Mater.* **2001**, *13*, 1649; b) G. Ibarz, L. Dahne, E. Donath, H. Mohwald, *Adv. Mater.* **2001**, *13*, 1324; c) S. Neyret, B. Vincent, *Polymer* **1997**, *38*, 6129; d) T. Sawai, S. Yamazaki, Y. Ikariyama, M. Aizawa, *Macromolecules* **1991**, *24*, 2117; e) B. E. Rodriguez, M. S. Wolfe, M. Fryd, *Macromolecules*

1994, *27*, 6642; f) B. R. Saunders, H. M. Crowther, B. Vincent, *Macromolecules* **1997**, *30*, 482.
[9] a) R. H. Pelton, P. Chibante, *Colloids Surf.* **1986**, *20*, 247; b) H. G. Schild, *Prog. Polym. Sci.* **1992**, *17*, 163; c) T. G. Park, A. S. Hoffman, *Biotechnol. Prog.* **1994**, *10*, 82–86; d) L. Y. Chu, S. H. Park, T. Yamaguchi, S. Nakao, *J. Membr. Sci.* **2001**, *192*, 27; e) L. Y. Chu, S. H. Park, T. Yamaguchi, S. Nakao, *Langmuir* **2002**, *18*, 1856; f) H. Vihola, A. Laukkaned, J. Hirvonen, H. Tenhu, *Eur. J. Pharm. Sci.* **2002**, *16*, 69.
[10] J. Ugelstad, A. Berge, T. Ellingsen, O. Aune, L. Kilaas, T. N. Nilsen, *Makromol. Chem. Macromol. Symp.* **1988**, *17*, 177.
[11] a) K. W. Hampton, W. T. Ford, *Macromolecules* **2000**, *33*, 7292; b) T. Miyata, N. Asami, T. Uragami, *Macromolecules* **1999**, *32*, 2082; c) F. Sauzedde, A. Elaissari, C. Pichot, *Colloid Polym. Sci.* **1999**, *277*, 1041; d) X. B. Ding, Z. H. Sun, G. X. Wan, Y. Y. Jiang, *React. Funct. Polym.* **1998**, *38*, 11.
[12] a) Y. H. Deng, W. L. Yang, C. C. Wang, S. K. Fu, *Adv. Mater.* **2003**, *15*, 1729; b) L. S. Zha, Y. Zhang, W. L. Yang, S. K. Fu, *Adv. Mater.* **2002**, *14*, 1090.
[13] Y. Lu, Y. Yin, B. T. Mayers, Y. Xia, *Nanoletters* **2002**, *2*, 183.
[14] B. Chu, Z. Wang, J. Yu, *Macromolecules* **1991**, *24*, 6832.
[15] a) C. Wu, S. Zhou, *Macromolecules* **1997**, *30*, 574; b) D. Gan, L. A. Lyon, *J. Am. Chem. Soc.* **2001**, *123*, 8203.
[16] M. Mary in *Scientific and Clinical Applications of Magnetic Carriers* (Eds.: U. Hafeli, W. Schutt, M. Zborowski), Plenum Press, New York, **1997**.
[17] a) A. Imhof, M. Megens, J. Engelberts, J. D. T. N. de Lang, R. Sprik, W. L. Vos, *J. Phys. Chem. B* **1999**, *103*, 1408; b) Z. Grauer, D. Avnir, S. Yariv, *Can. J. Chem.* **1984**, *62*, 1889.
[18] N. Peppas, P. L. Ritger, *J. Controlled Release* **1987**, *5*, 23.
[19] R. Massart, V. Cabuil, *J. Chim. Phys. Phys.-Chim. Biol.* **1987**, *84*, 967.
[20] A. van Blaaderen, A. Vrij, *Langmuir* **1992**, *8*, 2921.

Received: May 30, 2005
Published online: July 27, 2005

